

PAPER

An undergraduate laboratory experiment for measuring ϵ_0 , μ_0 and speed of light c with do-it-yourself catastrophe machines: electrostatic and magnetostatic pendula

To cite this article: Todor M Mishonov *et al* 2017 *Eur. J. Phys.* **38** 025203

View the [article online](#) for updates and enhancements.

Related content

- [Simple do-it-yourself experimental set-up for electron charge \$e\$ measurement](#)
T M Mishonov, E G Petkov, N Zh Mihailova *et al.*
- [Gravitational deflection of light and massive particle by a moving kerr-newman black hole](#)
Guansheng He and Wenbin Lin
- [CATASTROPHE VERSUS INSTABILITY FOR THE ERUPTION OF A TOROIDAL SOLAR MAGNETIC FLUX ROPE](#)
B. Kliem, J. Lin, T. G. Forbes *et al.*

Recent citations

- [Simple do-it-yourself experimental set-up for electron charge \$e\$ measurement](#)
T M Mishonov *et al*



IOP | ebooks™

Bringing you innovative digital publishing with leading voices to create your essential collection of books in STEM research.

Start exploring the collection - download the first chapter of every title for free.

An undergraduate laboratory experiment for measuring ε_0 , μ_0 and speed of light c with do-it-yourself catastrophe machines: electrostatic and magnetostatic pendula

Todor M Mishonov^{1,4}, Albert M Varonov¹,
Dejan D Maksimovski², Stojan G Manolev³,
Vassil N Gourev¹ and Vasil G Yordanov¹

¹ Department of Theoretical Physics, Faculty of Physics, St. Clement of Ohrid University at Sofia, 5 James Bourchier Blvd., BG-1164 Sofia, Bulgaria

² Private Yahya Kemal High School Skopje—Butel, Butelska bb. Blvd, MKD-1000 Skopje, Macedonia

³ Middle School Goce Delchev, Purvomaiska str. 3, MKD-2460 Valandovo, R. Macedonia

E-mail: mishonov@gmail.com, avaronov@phys.uni-sofia.bg, dejan_maksimovski@yahoo.com, manolest@yahoo.com, gourev@phys.uni-sofia.bg and vasil.yordanov@gmail.com

Received 18 May 2016, revised 7 November 2016

Accepted for publication 30 November 2016

Published 22 December 2016



CrossMark

Abstract

An experimental set-up for electrostatic measurement of ε_0 , separate magnetostatic measurement of μ_0 and determination of the speed of light $c = 1/\sqrt{\varepsilon_0\mu_0}$ according to Maxwell's theory with percent accuracy is described. No forces are measured with the experimental set-up, therefore there is no need for a scale, and the experiment cost of less than £20 is mainly due to the batteries used. Multiplied 137 times, this experimental set-up was given at the Fourth Open International Experimental Physics Olympiad (EPO4) and a dozen high school students performed successful experiments. The experimental set-up actually contains two different pendula for electric and magnetic measurements. In the magnetic experiment the pendulum is constituted by a magnetic coil attracted to a fixed one. In the electrostatic pendulum when the distance between the plates becomes shorter than a critical value the suspended plate catastrophically sticks to the fixed one, while in the magnetic pendulum the same occurs when the current in the coils becomes

⁴ Author to whom any correspondence should be addressed.

greater than a certain critical value. The basic idea of the methodology is to use the loss of stability as a tool for the determination of fundamental constants.

Keywords: vacuum electric permittivity, vacuum magnetic permeability, pendulum, catastrophic machine, speed of light, canonical fold catastrophe

(Some figures may appear in colour only in the online journal)

1. Introduction

From a metrological point of view the speed of light is a fixed constant $c = 299\,792\,458\,\text{ms}^{-1}$ [1]. The same can be said for the magnetic permeability constant $\mu_0 = 4\pi \times 10^{-7}\,\text{NA}^{-2}$. The electric permittivity ‘of the vacuum’ is also a matter of definition $\varepsilon_0 = 1/(4\pi c^2 \times 10^{-7})\,\text{Fm}^{-1}$. However, the measurement of the speed of light marks one important milestone in the development of physics. In this epoch, when Maxwell introduced his term $\mu_0\varepsilon_0\partial_t\mathbf{E}$ in the displacement current, he understood that speed of light can be determined by two separate static experiments for measurement of μ_0 , ε_0 and subsequently $c = 1/\sqrt{\varepsilon_0\mu_0}$. [2]. In our work we describe two different electric and magnetic set-ups.

But as in biology the individual development repeats the evolutionary one, so when the present-day students ‘measure’ ε_0 and μ_0 they are greeted with ‘Congratulations, you have just measured one of the fundamental constants of nature!’ [3] but not ‘Your multimeter is still OK!’. The same goes for Berkeley, California [4], the Balkan peninsula for University of Sofia student lab practicum [5] and for high school matriculation in Breziche [6].

The purpose of the present work is to suggest a simple set-up for measurement of the speed of light with 1% accuracy using the idea from catastrophe theory. Our set-up is inspired by the work of Tim Poston’s ‘Do-it-yourself catastrophe machine’ [7] and was reproduced 137 times for the participants in the Fourth International Experimental Physics Olympiad (EPO4) [8].

2. Experimental set-up description

2.1. Electrostatic experiment

A preliminary experimental task is to measure the voltage source \mathcal{E} with a calibrated multimeter (figure 1). For the set-up given to the high school students we used 12 V (23A type) batteries placed in PVC plumbing tubes along with a 1 M Ω resistor limiting the current [8].

By series connecting groups of eight 12.5 V batteries and mounting each group in PVC plumbing tubes, we have available sources of emf in multiples of 100 V to a maximum of 400 V. However for the determination of \mathcal{E} , according to figure 2, the internal resistance of the voltmeter r_V , which is comparable to the protective resistance r_{load} , had to be accounted for. A task from the experiment required the internal resistance of the voltmeter to be measured by the students. For the multimeters used, see figure 1, the internal resistance in voltmeter mode is 1 M Ω . The general set-up is depicted in figure 3.

The voltage is applied to the plates of the capacitor, which are parallel and coaxial. If initially the distance between the plates is x , upon the electric force action the pendulum is shifted towards the wooden block to a distance $x - z$ and the distance between the plates now is $z(x)$, as is shown in figure 4; this distance is much smaller than the plate diameter $z \ll D_e = 2R_e$ and if we neglect the capacitor effects of ends, the plate capacitor capacitance

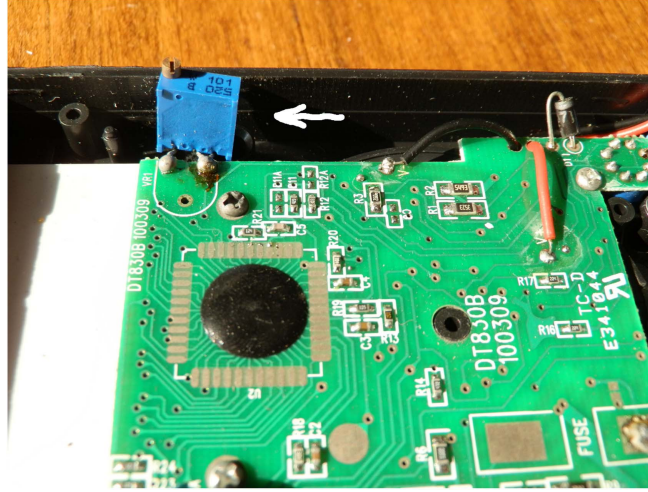


Figure 1. A photograph of an open multimeter DT830B showing the trimmer added for calibration (indicated by the arrow). The manufacturer <http://all-sun.com/> omitted the calibrating trimmer, and the author of the text and the organizers of the Experimental Physics Olympiad soldered 137 trimmers to the multimeters and calibrated the latter to the nominal 1% accuracy announced in the manual http://all-sun.com/manual/Dt830_en.pdf. The position of the omitted trimmer resistor can be easily seen in the corner of the PCB (printed circuit board). The terminals of the added trimmer to be soldered are the central one and one of the extremes. Some substandard multimeters are produced by substitution of the resistive trimmer by a constant typically a 200 Ω SMD resistor [9]. After the calibration, the back enclosures were reinserted in place and screwed.

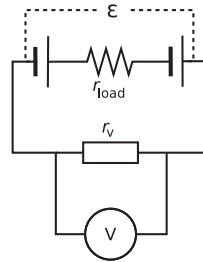


Figure 2. Schematics of the voltage source measurement given as a task to the participants in EPO4 [8]. The protective resistance r_{load} is placed among the batteries inside the PVC tube.

is $C = \epsilon_0 S/z$, where $S = \pi R_e^2$ is the plate area and ϵ_0 is the dielectric constant. The electric field between the capacitor plates is $E = \mathcal{E}/z$ and the opposite charges $Q = C\mathcal{E}$ accumulated in the plates create the attractive force

$$F_e = -\frac{1}{2}QE = P_e S = -\frac{1}{2}\epsilon_0 E^2 S, \quad P_e = -\frac{1}{2}\epsilon_0 E^2, \quad (1)$$

which is equal to the negative pressure of the Maxwell tensor times the plate area.

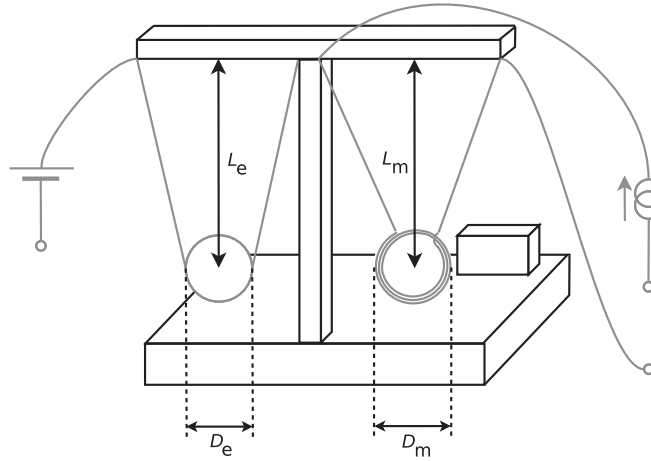


Figure 3. General scheme of the experimental set-up for ε_0 and μ_0 measurement, not to scale. The suspended capacitor plate is on the left-hand side of the T-shaped stand (made from two 13×10 mm wood bars (linden), 600 mm high and 400 mm across) and the suspended coil is on the right-hand side. The T-shaped stand is mounted on a wooden board measuring 400 mm in length, 200 mm in width and 17 mm in height. The plate D_e and coil D_m diameters are marked underneath, as well as the corresponding pendulum lengths L_e for the plate and L_m for the coil. The wooden block is depicted on the right without the capacitor plate fixed to it and the coil on opposite sides. A photograph of the block with all its components is given in figure 5. The emf symbol (batteries) is on the left of the suspended plate and connected to it. Analogously, the symbol of the current source is shown on the right of the suspended coil and connected to it. A photograph of the experimental set-up is given in [8].

Whereas the weight of the suspended plate $m_e g$ creates a projection of the force

$$F_g = +m_e g \frac{x - z}{L_e} \quad (2)$$

acting in the opposite direction, where L_e is the pendulum length for the electric experiment and analogously L_m is the pendulum length for the magnetic experiment, see figure 3. The total force

$$F(z) = F_e(z) + F_g(z) = -\frac{\partial}{\partial z} U_e(z)$$

can be represented as a derivative of the effective potential energy

$$U_e(z) = \frac{1}{2} \frac{m_e g}{L_e} (x - z)^2 - \frac{1}{2} \frac{\varepsilon_0 S \mathcal{E}^2}{z}.$$

The force balance determines the equilibrium position z_0

$$F(z_0) = -\frac{\partial}{\partial z} U_e \Big|_{z=z_0} = \frac{m_e g}{L_e} (x - z_0) - \frac{\varepsilon_0 S \mathcal{E}^2}{2z_0^2} = 0 \quad (3)$$

and the potential energy second derivative

$$k_e(z_0) \equiv -\frac{\partial^2}{\partial z^2} U_e \Big|_{z=z_0} = \frac{m_e g}{L_e} - \frac{\varepsilon_0 S \mathcal{E}^2}{z_0^3} = 0$$

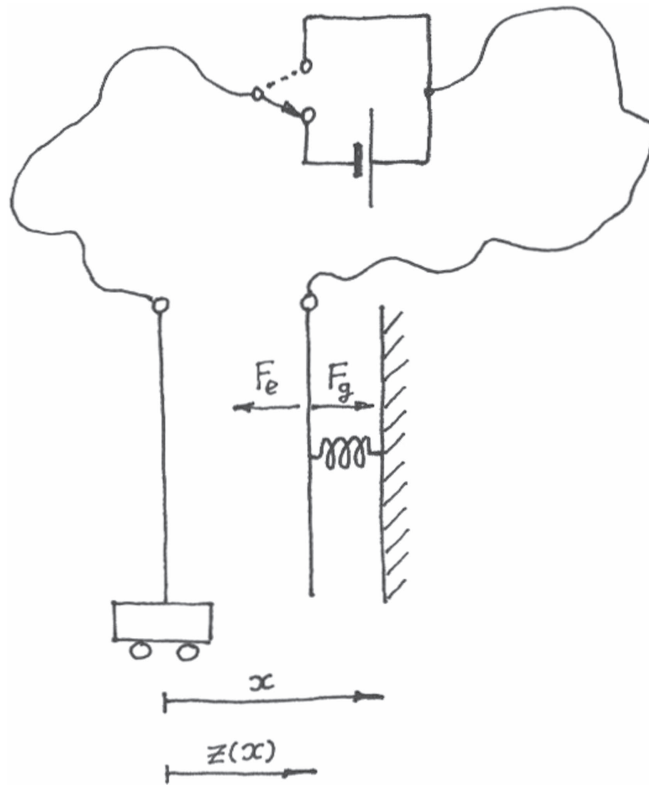


Figure 4. Scheme of the method for electrostatic measurement: a picture of the experimental set-up is given in the EPO4 problem. Under the action of the electric field created by the batteries, the movable plate of the capacitor deforms the spring with effective rigidity $\kappa = m_e g / L_e$. In equilibrium position $z(x)$ ‘the elastic force’ $F_g = \kappa(x - z)$ is compensated by the electric force $F_e = -\frac{1}{2}\epsilon_0 E^2 S$, $E = \mathcal{E}/z$, $S = \pi R_c^2$. We prefer an expression in which one can easily trace the origin of the different multipliers. We gradually decrease x and at some critical value x_c the equilibrium position $z_c \approx \frac{x_c}{3}$ loses stability and a catastrophe happens. The pendulum (the suspended plate of the capacitor) suddenly sticks to the fixed one at $z = 0$. When the switch is changed to the upper position, the pendulum minimizes its gravitational energy $\frac{\kappa}{2}(x_c - z)^2$ only and $z = x_c$. In a good approximation $x_c^3 \propto \mathcal{E}^2$, see equation (7). In the magneto-static experiment the plates are substituted with coils with parallel currents and $x_c^2 \propto I^2$, see equation (9).

determines whether this equilibrium is stable. For small deviations from the equilibrium positions we have

$$F(z) \approx -k_e(z_0)(z - z_0),$$

equivalent to Hooke’s law. For $k_e(z_0) > 0$ with negligible friction the pendulum frequency is $\omega^2 = k_e(z_0)/m_e$. This is the case of large enough distances between the block (figure 5) and the suspended pendulum. The most important part of the experiment is the slow and gradual approach of the block towards the pendulum, waiting for the oscillations to attenuate. A gradual increase in the pendulum period $T(z) = 2\pi/\omega$ is felt when the distance x reaches its critical value x_0 . In this critical position

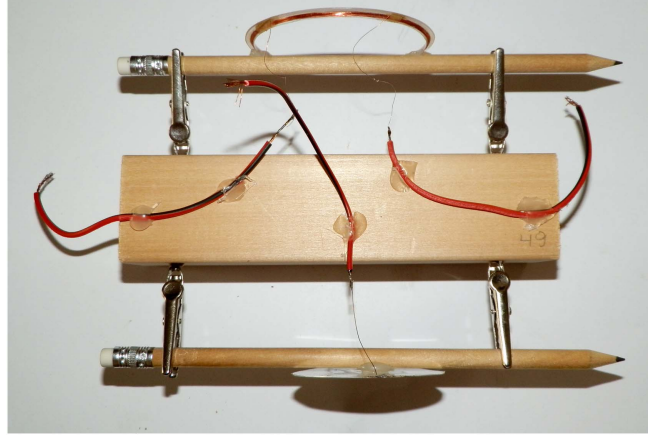


Figure 5. Top view photograph of the wood block for both experiments. A photograph of the whole set-up can be found in [8]. The plate of the capacitor is fixed to the lower pencil and the coil is fixed to the upper pencil. Both capacitor plate and coil are glued by hot melt adhesive to the pencils. Two ‘crocodiles’ hold each pencil to the wood block. The block is moved by hand. The use of the block and the experiment are schematically presented in figure 4.

$$k_e(z_0, x_0) = 0 \quad (4)$$

the equilibrium becomes indifferent and upon further decrease of $x < x_0$ the capacitor plates stick to each other, and the critical distance is determined from the solution of the system equations (3) and (4)

$$F(z_0) = 0, \quad \text{and} \quad k_e(z_0) = 0. \quad (5)$$

From the second equation we find z_0 and substituting in the first one we determine x_0 and thus we get the solution

$$\varepsilon_0 \mathcal{E}^2 = \mathcal{F}_e = \frac{32}{27\pi} \frac{m_e g x_0^3}{L_e D_e^2} (1 - f_e), \quad f_e \approx \frac{4}{3\pi} \frac{x_0}{D_e} \ll 1, \quad (6)$$

where the small correction f_e derived in the [10]. The slope of the linear regression can be easily evaluated as the ratio of the maximal equilibrium distance x_e (when the error is minimal) and corresponding maximal applied voltage \mathcal{E} . Then omitting the correction f_e , we obtain ε_0 from equation (6) directly expressed by measurable quantities only

$$\varepsilon_0 \approx \frac{32}{27\pi} \frac{m_e g x_e^3}{L_e D_e^2 \mathcal{E}^2}, \quad (7)$$

or in a good approximation $x_e^3 \propto \mathcal{E}^2$. Experimentally after carefully reaching the loss of stability, we interrupt the voltage supply and short-circuit the capacitor plates. After waiting for the pendulum oscillations to attenuate, we carefully measure the equilibrium distance x_0 between the pendulum plate and the plate fixed to the block by a pencil and two ‘crocodiles’, see figure 5. In such a way the right-hand side of equation (6) is expressed by experimentally determined parameters. For each value of the voltage \mathcal{F}_e is different but the coefficient of \mathcal{E}^2 is exactly the needed dielectric constant ε_0 . The experimental data of \mathcal{F}_e versus \mathcal{E}^2 is represented in tabular form in table 1 and graphically in figure 6.

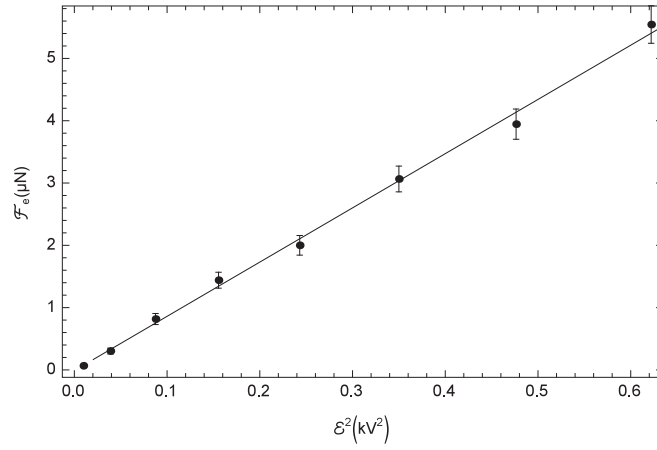


Figure 6. The linear regression \mathcal{F}_e versus \mathcal{E}^2 of the experimental data from table 1 according to equation (6). The slope of the line is $(8.7 \pm 0.2) \times 10^{-12} \text{ NV}^{-2}$, i.e. standard error/estimate = 2.3%; correlation coefficient = $0.9984 = 1 - 1.6 \times 10^{-3}$.

Table 1. Experimental data from the electrostatic experiment. For the plate mass and diameter, and pendulum length we have correspondingly $m_e = 1.14 \text{ g}$, $D_e = 54 \text{ mm}$, $L_e = 574 \text{ mm}$. The parasite computer generated extra digits are not rounded.

$x_0 \text{ (mm)}$	$x_0^3 \text{ (mm}^3\text{)}$	x_0/D_e	f_e	$\mathcal{F}_e \text{ (mN)}$	$\mathcal{E} \text{ (V)}$	$\mathcal{E}^2 \text{ (V}^2\text{)}$
3	27	0.056	0.0236	6.65×10^{-5}	98.7	9.74×10^3
5	125	0.093	0.0393	3.03×10^{-4}	197.2	38.9×10^3
7	343	0.130	0.0550	8.17×10^{-4}	295.9	87.6×10^3
8.5	614	0.157	0.0668	1.45×10^{-3}	394.3	155×10^3
9.5	857	0.176	0.0747	2.00×10^{-3}	493.0	243×10^3
11	1331	0.204	0.0865	3.07×10^{-3}	591.6	350×10^3
12	1728	0.222	0.0943	3.95×10^{-3}	690.2	476×10^3
13.5	2460	0.250	0.1061	5.54×10^{-3}	788.7	622×10^3

2.2. Magnetostatic experiment

Here we use a slightly different method; the corresponding scheme is given in figure 7. Initially we fix the distance x and increasing the electric current I through the attracting coaxial coils, observe the gradual loss of stability and at some critical current I_0 the coils stick to each other. The control variable in the magnetostatic experiment is the current, while in the electrostatic one the control variable is the distance x . Measuring the current I of the slow loss of stability, knowing the length of the pendulum L_m , the weight of the suspended coil $m_m g$, the number of turns N , and the diameter of the coils $D_m = 2R_m$, analogously to equation (6) we obtain

$$\mu_0 I^2 = \mathcal{F}_m \equiv \frac{m_m g x^2}{2L_m N^2 D_m} (1 + f_m), \quad f_m \approx \frac{1}{16} \left(-5 + 6 \ln \frac{8}{\delta} \right) \delta^2, \quad \delta \equiv \frac{x}{D_m} \ll 1. \quad (8)$$

Analogously to the electrostatic experiment and equation (7), we can express μ_0 from equation (8) omitting the correction f_m in measurable quantities

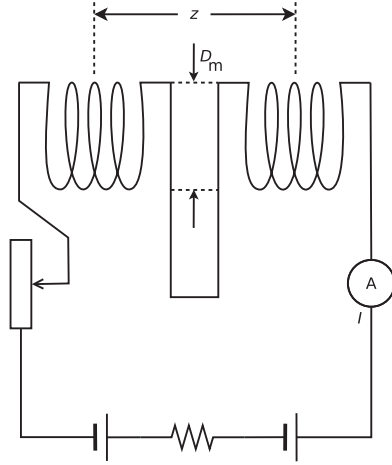


Figure 7. Top view of the magnetostatic experiment. An electric circuit is depicted here. The current from the batteries, measured by the amperemeter, passes through the coaxial coils with diameter D_m and distance between them z . The current is regulated by the variable resistor consisting of 1 m kanthal wire shown on the left of the scheme. A load resistor is given between the batteries which limits the current. The 64 mm diameter coils consist of 50 turns of 100 μm lacquered copper wire. For a photograph, see [8].

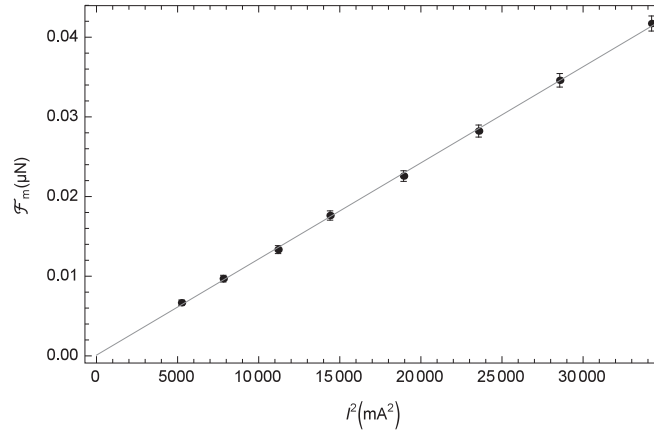


Figure 8. The linear regression \mathcal{F}_m versus I^2 of the experimental data from table 2 according to equation (8). The slope of the line is $(12.07 \pm 0.11) \times 10^{-7} \text{ NA}^{-2}$, i.e. standard error/estimate = 0.91%; correlation coefficient = $0.99976 = 1 - 2.4 \times 10^{-4}$.

$$\mu_0 \equiv \frac{m_m g x_m^2}{2L_m N^2 D_m I^2}, \quad \mu_0 \propto I^2. \quad (9)$$

In other words we determine μ_0 from the loss of stability criterion equation (5). Here x_m is the best measured maximal value of equilibrium distance and I is the corresponding current. Combining equations (7) and (9) we express the the speed of light c in measurable quantities

Table 2. Experimental data from the magneto-static experiment. For the coil mass and diameter, and pendulum length we have correspondingly $m_m = 1.18$ g, $D_m = 64$ mm, $L_m = 558$ mm.

x (mm)	x^2 (mm ²)	x/D_m	f_m	\mathcal{F}_m (mN)	I (mA)	I^2 (mA ²)
10	100	0.156	0.0284	6.67×10^{-6}	72.4	5.24×10^3
12	144	0.188	0.0385	9.70×10^{-6}	88.4	7.81×10^3
14	196	0.219	0.0496	1.33×10^{-5}	105.8	11.2×10^3
16	256	0.250	0.0617	1.76×10^{-5}	120	14.4×10^3
18	324	0.281	0.0746	2.26×10^{-5}	137.6	18.9×10^3
20	400	0.313	0.0882	2.82×10^{-5}	153.5	23.6×10^3
22	484	0.344	0.1025	3.46×10^{-5}	169	28.6×10^3
24	576	0.375	0.1174	4.17×10^{-5}	185	34.2×10^3

$$c \approx \left(\frac{27\pi}{16} \frac{L_m N^2 D_m I^2}{m_m g x_m^2} \frac{L_e D_e^2 \mathcal{E}^2}{m_e g x_e^3} \right)^{1/2}, \quad (10)$$

where x_e is the best measured equilibrium distance for the electrostatic experiment and x_m is the equilibrium distance for the magnetostatic experiment determined with the highest accuracy and \mathcal{E} and I are corresponding voltage and current.

The illustrative data obtained from our set-up is tabulated in table 2 and the linear regression \mathcal{F}_m versus I^2 shown in figure 8 determines μ_0 .

Having estimated ε_0 from figure 6 and μ_0 from figure 8, we calculate the speed of light $c = 3.086 \times 10^8$ m s⁻¹, which is less than 3% from the exact value, in agreement with the error estimations from both linear regressions. Better than 1% percent accuracy can be reached if we apply kV range voltages, which give larger electrostatic shifts for the corresponding pendulum.

As in the electrostatic problem, equation (8) is derived as the solution of the system

$$F_m(z) = -\frac{\partial}{\partial z} U_m(z, I) = 0, \quad \text{and} \quad k_m(z) \equiv \frac{\partial^2}{\partial z^2} U_m(z, I) = 0. \quad (11)$$

The total magnetic force

$$F_m(z) = \frac{m_m g}{L_m} (x - z) - 2 \frac{\mu_0}{4\pi} (IN)^2 2\pi R_m \frac{1}{z} = 0 \quad (12)$$

is derived supposing that the conductors are infinite and parallel. Actually, the magnetic field of a circular coil is given in every textbook in electrodynamics but technical details containing approximate formulae with elliptic integrals are given in the unabridged version of the present work [10]; such horrible math is a deterrent for the readers of contemporary journals. Nevertheless colleagues involved with construction of new experimental set-ups have to be able to use this concise, sequential and reproducible derivation of the correction function used in the present work. In principle, the determination of μ_0 can also be given by changing the position of the block at a fixed current, as in the electrostatic experiment. The common idea of these different experiments is described in the next section where we analyse the fold of the potential energy.

The initial idea was to use not two pendula but a single one in which we have simultaneously: a plate of the capacitor and a coil wound around the perimeter, and the same

structure affixed to the wood block. Having the pendulum length L and mass m , for the speed of light from equation (10) we have

$$c \approx N \frac{I\mathcal{E}}{mg} \sqrt{\frac{27\pi}{16} \frac{D^3 L^2}{x_e^3 x_m^2}}, \quad (13)$$

where the dimensionality of the right-hand side is obvious. The catastrophe theory allowed us to obtain this simple formula.

The pendulum unification requires higher voltage values that are dangerous for operation by high school students and that is precisely the main reason for not implementing this idea.

2.3. Experimental uncertainty estimation

The experimental data processing requires linear regression both for the electric and magnetic experiments. Here we will not repeat the well known formulae for the uncertainty of the coefficient of the linear regression and the correlation coefficient. However, the relative uncertainty of the slopes gives the best evaluation of the accuracy of our experiments. With the described setup 1% accuracy is reachable. Here we have to comment on evaluation of the measuring errors and their effect on the final result. Some factors have to be described only qualitatively. For example, analytical scales are in glass boxes while our setup is not screened. That is why the windows and doors have to be closed and also breathing should be not very intensive. Vice versa, it is difficult to evaluate the influence of the turbulence from a long nose to the fold point of the canonical catastrophe. The geometry of the system is quite good and the main source of error is the measurement of distances x with accuracy of 1/2 mm. In such a way the error is less than 0.25 mm, which for a distance of 10 mm gives an error of 2.5%. Making $N = 10$ measurements $1/\sqrt{N}$ factor reduces the error below 1%. Having a dominant source of errors, it is senseless to analyze the other negligible ones. For small relative errors of the determined speed of light and significant deviation from the known value we have to look for systematic errors, for example, to check the calibration of the multimeter or to check the number of the turns of the coil. The linear regression relative errors are given in the captions of figure 6 for ε_0 and figure 8 for μ_0 .

3. Additional considerations

At a fixed voltage \mathcal{E} for the electrostatic experiment or a fixed current I for the magnetostatic one, the potential energy depends on two parameters z and x . The position of the block x controls the stability of the system and its behaviour with respect to small perturbations. In this sense x is a control parameter. The idea of our experiment is by a slow decrease of the control parameter to determine the critical value x_c at which the system changes its behaviour and the potential minimum disappears. The system suddenly changes its state from stable minimum at z_c to collapsed plates or coils with $z = 0$. At the critical point (z_c, x_c) we have a system describing the loss of stability, such as equation (5) for the electric experiment and equation (11) for the magnetic experiment

$$\partial_z U(z_c, x_c) = 0, \quad \text{and} \quad \partial_z^2 U(z_c, x_c) = 0.$$

In the proximity of this critical point of loss of stability for the potential energy we have

$$U \approx U_c + U_{zx}(z - z_c)(x - x_c) + \frac{1}{3!} U_{zzz}(z - z_c)^3, \quad (14)$$

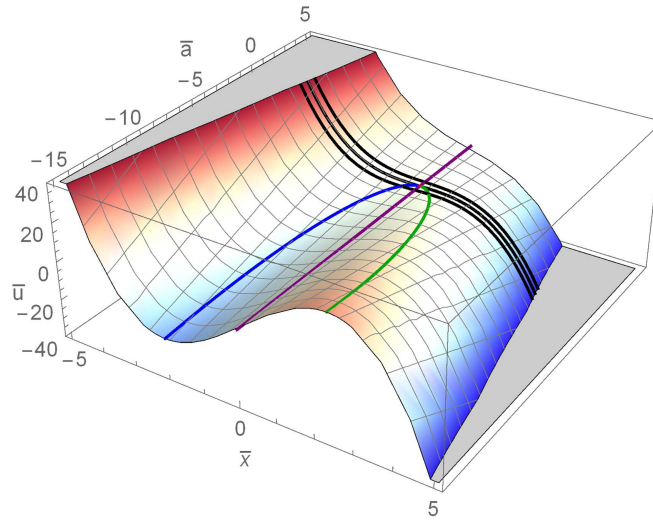


Figure 9. Fold of potential energy according to equation (16). Parabola of extrema is described by equation (19). The straight line $\bar{x} = 0$ describes the zeros of the second derivative (inflex line) of \bar{u} with respect to \bar{x} . Minima and maxima merge in the critical point of the fold catastrophe (0, 0, 0). The inflex line also passes through this critical fold point and alongside with the parabola of the extrema, form a ψ -shaped cross. At a fixed \bar{a} the disappearance of the extrema is described by the three parallel curves. The methodology of our experiment is as follows: starting from a minimum of \bar{u} with respect to \bar{x} at fixed negative $\bar{a} < 0$, we slowly increase the only control variable \bar{a} until the critical value $\bar{a} = 0$ is reached, where the system from the fold point plunges down in the precipice along the middle curve. See equation (5.4) and figure 5.6 in [12]. See how the hand drawing is much more expressive than the contemporary computer graphics.

where

$$U_c = U(z_c, x_c), \quad U_{zx} = \partial_z \partial_x U(z_c, x_c) < 0, \quad U_{zzz} = \partial_z^3 U(z_c, x_c) > 0.$$

Let us introduce new variables

$$\bar{x} \equiv z - z_c, \quad \bar{u} \equiv -\frac{3!(U - U_c)}{U_{zzz}}, \quad \bar{a} \equiv \frac{3!U_{zx}}{U_{zzz}}(x - x_c), \quad (15)$$

\bar{x} is the variable of the state of the system or behaviour variable, \bar{a} is the only control parameter of the system, and \bar{u} is the dimensionless potential energy which should be minimal $\bar{u}(\bar{x}; \bar{a})$.

In these new variables, the approximate Taylor expansion for the fold of the potential energy equation 14 takes the universal form

$$\bar{a} \bar{x} + \bar{x}^3 + \bar{u} = 0, \quad (16)$$

depicted in figure 9. In our problem \bar{u} is proportional to the potential energy of the system. The control parameter is only \bar{a} corresponding to the current or voltage, and \bar{x} represents the displacement of the pendulum from the critical point of loss of stability.

Let us analyze other physical systems which are described with the same mathematics. Formally the left-hand side of equation (16) is a derivative

$$\bar{a} \bar{x} + \bar{x}^3 + \bar{u} = \frac{dV_{ab}}{d\bar{x}}, \quad V_{ab}(\bar{x}) = \frac{1}{4}\bar{x}^4 + \frac{1}{2}\bar{a} \bar{x}^2 + \bar{u} \bar{x}. \quad (17)$$

In the Landau theory of second order phase transitions $V_{ab}(\bar{x})$ is the free energy or thermodynamic potential as a function of the order parameter \bar{x} , \bar{a} is the reduced temperature and \bar{u} is the external field. From the point of view of Landau theory equation (16) is the equation for the equilibrium value of the order parameter (or locus of equilibria or surface of equilibrium) \bar{x} , see equation (V.144.4) in the Landau–Lifshitz [11] course. On the other hand in the sense of our problem \bar{u} is the potential energy of the system.

The mathematical theory of catastrophe systematizes similar types of problems. As a reference book we will address the monographs by Poston and Stewart [12]. According the terminology of this book $V_{ab}(\bar{x})$ is called the potential function (chapter 5, section 2), and the surface

$$V_a(\bar{x}) = \frac{1}{3}\bar{x}^3 + \bar{a} \bar{x}, \quad \bar{a} = 3\bar{a}, \quad \bar{u} = -3V_a, \quad \bar{a} \bar{x} + \bar{x}^3 + \bar{u} = 0, \quad (18)$$

corresponding after an obvious change of variables to our equation (16) is called fold catastrophe. Unfortunately there is no figure presenting the surface $V_a(\bar{x}, \bar{a})$ in (V_a, \bar{x}, \bar{a}) space in this book, which is why we refer to other figures having the same shape but different meaning of the variables. Further we will cite equivalent figures and equations from the reference book by Poston and Stewart even if the terminology is different; for example, our equation (16) is equation (5.2) [12, chapter 5, section 2].

For our problem the potential energy U is proportional to the potential function $V_a(x)$ of the canonical fold catastrophe and equation (16) describes the potential surface (figure 9); by the way this is the situation of a particle orbiting around a black hole [11], again a fold catastrophe. However for the physics of a second order phase transition equation (16) describes the locus of equilibria for the order parameter and two control parameters: reduced temperature [11] and external magnetic field for the example of the physics of the ferromagnets; it is the so called canonical cusp catastrophe.

The described experiments and their theory can be carried out and understood without knowing catastrophe theory. However, for a deep understanding we wish to know why the loss of stability of electric and magnetic experiments is approximately described by one and the same universal surface, which also describes many other physical situations. Last but not least, our work was inspired by the catastrophe theory and that is precisely the relation of the experiment to the catastrophe theory. We wish to popularize in experimental physics a rich system of notions and ideas, actually coming again from physics.

The extrema of the surface $\bar{u}(\bar{x}; \bar{a})$ obey the equation

$$d_{\bar{x}}\bar{u} = -3\bar{x}^2 - \bar{a} = 0 \quad (19)$$

with the solutions $\bar{x} = \pm\sqrt{(-\bar{a})/3}$, for $\bar{a} < 0$. The minimum at $\bar{x} = -\sqrt{(-\bar{a})/3}$ gives

$$\bar{u} = -\frac{2}{3^{3/2}}(-\bar{a})^{3/2} < 0$$

and the maximum at $\bar{x} = +\sqrt{(-\bar{a})/3}$ gives

$$\bar{u} = +\frac{2}{3^{3/2}}(-\bar{a})^{3/2} > 0.$$

The extrema are described by the common equation (equation 5.3 of [12])

$$27\bar{u}^2 + 4\bar{a}^3 = 0. \quad (20)$$

The most essential part of our experiment is the slow trace of the disappearance of the stable minimum when the control variable \bar{a} reaches the critical value. In the fold point the state variable \bar{x} suddenly changes its behaviour in a catastrophic manner, i.e. the pendulum sticks to the fixed plate or coil.

The pendulum transition, which at a critical value of the current I , voltage \mathcal{E} or the distance from equilibrium x suddenly rushes towards the block, is an example of the so called catastrophic jumps by René Thom [13] and Cristopher Zeeman [14]. The variables x , \mathcal{E} or I are called control variables (or control parameters) and z is called a behaviour variable (or state variable). The catastrophic jumps occur when smooth variations of controls cause a discontinuous change of state. In other words, the variable x is a control parameter and the distance z between the coils or capacitor plates is a behaviour variable. The variable z has a catastrophic change when a smooth variation of x takes place around the critical value x_c . Without referring the catastrophe theory notions explicitly, such behaviour can be found in many physical problems: stability of orbits in the field of a black hole, appearance of p-, d-, f-, and g-electrons in atoms with different Z , critical point, corresponding states rule and Landau theory of second order phase transitions, plane flow of compressional gases, see the well-known Landau and Lifshitz course [11], and also recently for eruptive phenomena in the solar atmosphere [15]. And there are applications in such fields as heartbeat and propagation of a nerve impulse [16, 17]. Landau concepts of the description of a phase transition by breaking the symmetry order parameter replaced the science of type of zoology with a unified theory [18]. It is interesting that even biological phenomena can be described by differential equations similar to the kinetics of the order parameter [11]. Having only one control parameter, i.e. voltage or current, the theoretical analysis is trivial and we obtain the canonical fold. That is why our work is purely experimental. One of the purposes of our article is to activate the system of notions of the catastrophe theory, which can be useful for the analysis of much experimental research. After all, the experimental physics is a mental activity.

Our experimental set-up is to a large extent influenced by the Zeeman catastrophe machine [14] and by Tim Poston's work on the 'Do-it-yourself catastrophe machine' [7]. In our machine the rubber elastics are replaced by force lines of the electric and magnetic field, in the same intuitive manner in which Faraday introduced force lines and concepts of a field in mathematical physics. The Do-it statement does not refer to funding restrictions; we introduce a new idea for the use of catastrophe theory in the methodology of a student laboratory.

The theory of the described experiment is related to analysis of the potential surfaces for the electric W_e and magnetic W_m problems. The detailed theoretical derivation can be found in [10]. In figure 11 the potential surfaces are depicted in dimensionless variables

$$W_e(Z, X) = \frac{1}{2}(X - Z)^2 - \frac{1}{2Z}, \quad X = \frac{x}{a}, \quad Z = \frac{z}{a},$$

$$\varkappa \equiv \frac{m_e g}{L_e}, \quad W \equiv \frac{U_e}{\varkappa a^2}, \quad a^3 \equiv \frac{\varepsilon_0 S \mathcal{E}^2}{\varkappa}, \quad (21)$$

$$W_m(Z, X) = \frac{1}{2}(X - Z)^2 + \ln Z, \quad X = \frac{x}{b}, \quad Z = \frac{z}{b},$$

$$\varkappa \equiv \frac{m_m g}{L_m}, \quad W \equiv \frac{U_m}{\varkappa b^2}, \quad b^2 \equiv \frac{\mu_0 R_m (NI)^2}{\varkappa}. \quad (22)$$

The sections $W(Z, X)$ in figure 12 are given for three typical section values $W(Z, X)$ for $X < X_c$, $X = X_c$ and $X > X_c$.

For a logically connected derivation and introduction of dimensionless variables X , Z and W , see [10].

4. Discussion and conclusions

This experimental set-up is part of the Physics Faculty of St. Clement of Ohrid University program for the development of cheap experimental set-ups for fundamental constant measurements, see for example the description of the set-up for measurement of the Planck constant by electrons [19] and the measurement of the speed of light by analytical scales [5]. The experimental set-ups can be constructed even in high (secondary) school laboratories and the corresponding measurements can be conducted by high (secondary) school students. The authors are grateful to the 137 participants (students and teachers) in EPO4, where the described experimental set-up in this article was used and a dozen students measured c and derived the formulas [8]. Every description of an experimental set-up contains obligatory accessories, such as a technical specification, drawings, photos, tables, figures, evaluation of errors, etc, but the essence of our work is the introduction of new ideas. In general, we can conclude that the notions of catastrophe theory can be very useful for the invention of new set-ups in student physics laboratories. This is a style of thinking in broad problems in science and technology.

Acknowledgments

The Olympiad was held with the cooperation of the Faculty of Physics of St. Clement of Ohrid University at Sofia—special gratitude to the Dean, Professor A Dreischuh, and also to the President of the Macedonian Physical Society, Associate Professor B Mitrevski, and the President of the Balkan Physical Union Acad. A Petrov. Many thanks to the Bulgarian sponsors of the Olympiad, who ensured the manufacture of 137 copies of the experimental set-up. Special gratitude for their support and assistance in the organization of the Olympiad goes to Z Dimitrov, M Stoev, D Damyanov, A Petkov, S Velkov, A Bozhankova, P Beckyarov, D Todorov, L V Georgiev, P Bobeva, D Kocheva, A Stefanov, M Angelova, L Angelov, N Yordanova, Ts Metodieva, K Koleva, I Dimitrov, K Gourev, B Nathan, D Tsvetanov, L Atanasova, D Damyanov, A Vassileva, G Parkov, V Ivanova, R Simeonov, N Panaiotov, K Angelov, Associate Professor E Peneva and Associate Professor S Kolev.

We, the EPO4 organizers, are grateful to the high school participants who managed to derive the $\varepsilon_0 \mathcal{E}^2$ and $\mu_0 I^2$ formulas without the correction functions f_e and f_m .

The authors, including the EPO4 champion Dejan Maksimovski who measured the speed of light with 1% accuracy, are thankful to the university students from Skopje Biljana Mitreska and Ljupcho Petrov, who during the night after the experimental part of the Olympiad, solved a significant part of the correction functions f_e and f_m derived here and used for the accurate determination of ε_0 , μ_0 and c by the electrostatic and magnetostatic experiments.

Appendix A. Cuspoid of every regular space curve in the normal plane

In this appendix we will describe the line of minima and maxima depicted on the potential surface of figure 9 and their projections from figure 10. Let us describe an analogy. Take in your hands the cable of your PC and look along the tangent at some point of the cable. Let us

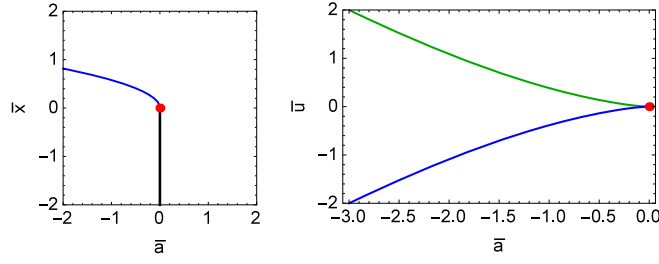


Figure 10. (Left) State variable \bar{x} as function of the control variable \bar{a} ; top view of figure 9. When increasing \bar{a} the minimum disappears and in the critical fold point the system catastrophically loses stability. The collapse is presented by a vertical line. For our setup the collapse means sticking of the coils of the magnetic pendulum, for example. The experimental observation of a fold point is the basis of our idea for determination of ε_0 , μ_0 and c in the undergraduate experiment. Confer the fold catastrophe map given in figure 9.1 in [12]. (Right) The semicubic curve given by equation (20). It is the $(\bar{a}-\bar{u})$ projection of extrema curves depicted in figure 9. The abscissa is the control parameter \bar{a} and the ordinate is the parameter \bar{u} , which is proportional to the potential energy of the system. Our methodology is related to the slow increase of \bar{a} moving along the lower curve of the minima; see figure 5.3 of [12]. Reaching the critical fold point ($\bar{a} = 0$, $\bar{u} = 0$), the system (the experimental set-up) catastrophically changes its behaviour. In the real experiment the vertical is the potential energy, while the horizontal is the distance in the electrostatic experiment and the current in the magnetostatic experiment. See the map depicted in figure 5.6 in [12]. In the $(\bar{a}-\bar{u})$ plane the fold point is at the corner of the semi-cubic parabola equation (20).

choose around some regular point of the curve the local x -axis along the tangent \mathbf{t} , y -axes along the normal \mathbf{n} , and z -axes along the binormal $\mathbf{b} = \mathbf{t} \times \mathbf{n}$. In this local system for the space vector we have

$$\begin{aligned} \mathbf{r}(s(t)) &= x\mathbf{t} + y\mathbf{n} + z\mathbf{b}, & x &= s, & y &= \frac{1}{2!}\bar{\kappa}s^2, \\ z &= \frac{1}{3!}\bar{\kappa}\tau s^3, & s &\ll \frac{1}{\sqrt{\bar{\kappa}^2 + \tau^2}}, \end{aligned} \quad (\text{A.1})$$

where s is the length along the curve. In the normal $(\mathbf{n}-\mathbf{b})$ plane we have

$$9\bar{\kappa}z^2 = 2\tau^2y^3, \quad (\text{A.2})$$

where $\bar{\kappa}$ is the curvature and τ is the torsion. For a constant vector \mathbf{V} in $(\mathbf{t}, \mathbf{n}, \mathbf{b})$ space, i.e. in the Frenet–Serret frame

$$\mathbf{V} = \alpha\mathbf{t} + \beta\mathbf{n} + \gamma\mathbf{b}, \quad \alpha = \text{const}, \quad \beta = \text{const}, \quad \gamma = \text{const}, \quad (\text{A.3})$$

the angular velocity is

$$\boldsymbol{\omega} = v(\bar{\kappa}\mathbf{b} + \tau\mathbf{t}), \quad v = \frac{ds}{dt}, \quad (\text{A.4})$$

where t (let us call it time) is an arbitrary parameter parametrising the curve and the length along the curve $s(t)$. For the time derivative of the vector we have

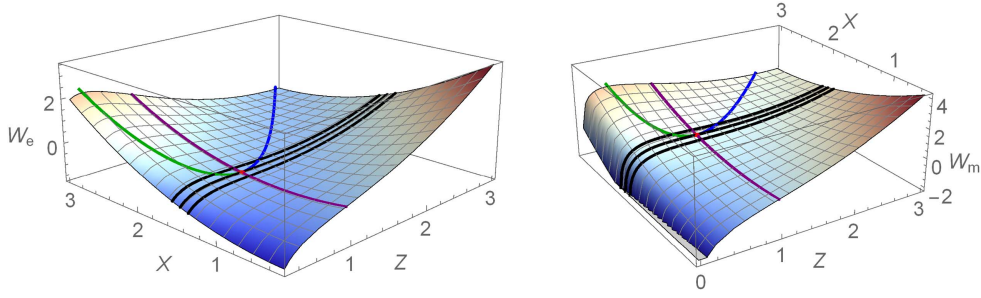


Figure 11. The potential surfaces W_e (left) and W_m (right). The right branch of the curves represents the stable local minima of the potential energy as function of Z at fixed values of X . The left branch of the curves shows the local unstable maxima. Those two branches join at the critical point at which the minima and maxima annihilate for the critical value X_c . The three parallel curves over both surfaces are copied in figure 12. Those curves demonstrate local extrema for $X > X_c$, monotonous dependence for $X < X_c$, and most importantly the catastrophic behaviour at the critical value $X = X_c$.

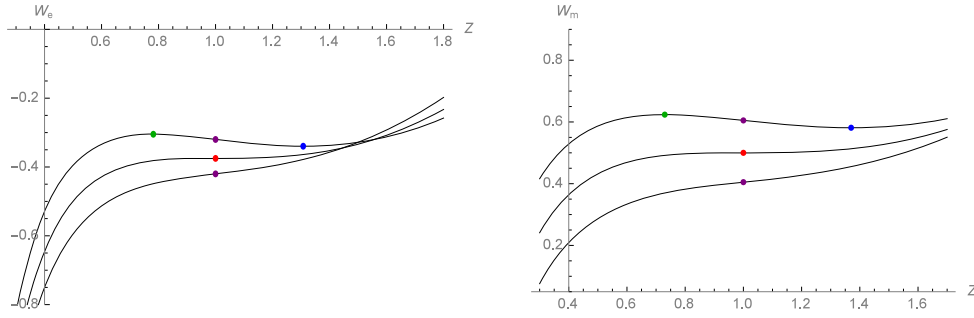


Figure 12. The sections of the potential surfaces close to the critical fold point for the electric W_e (left) and the magnetic W_m (right) problems. For the critical value $X = X_c$ maxima and minima merge in an inflection point. For $X < X_c$ the potential curves are monotonous without local extrema. The zeros of the second derivative between the minimum and the maximum of the potential curves are shown by a line forming the middle of the ψ -shaped peculiarity. Confer the fold curves in figure 5.6 of [12] and figure 11 for the electric and magnetic problem and the model universal surface figure 9 around the fold point.

$$\frac{d\mathbf{V}}{dt} = \boldsymbol{\omega} \times \mathbf{V}. \quad (\text{A.5})$$

Substituting here \mathbf{t} , \mathbf{n} , \mathbf{b} we have the Frenet–Serret formulae [20, 21]

$$\frac{d\mathbf{t}}{ds} = \overline{\kappa}\mathbf{n}, \quad \frac{d\mathbf{n}}{ds} = -\overline{\kappa}\mathbf{t} + \tau\mathbf{b}, \quad \frac{d\mathbf{b}}{ds} = -\tau\mathbf{n}. \quad (\text{A.6})$$

Finally the comparison of equation (19), equation (20), and equation (A.2) gives that for the standard canonical fold we have $\overline{\kappa} = 6$ and $\tau = 2$ for the line of the extrema in figure 9.

References

- [1] Mohr P J, Taylor B N and Newell D B 2012 CODATA recommended values of the fundamental physical constants: 2010 *Rev. Mod. Phys.* **84** 1527
- [2] Maxwell J C 1865 A dynamical theory of the electromagnetic field *Phil. Trans. R. Soc.* **155** 459–512
- [3] MIT OCW 2005 *Course 8.02T* http://ocw.mit.edu/courses/physics/8-02t-electricity-and-magnetism-spring-2005/labs/experiments_2_and_8
- [4] Purcell E M 1963 *Electricity and Magnetism (Berkeley Physics Course vol 2)* (New York: McGraw-Hill) problem 7.25, figure 7.42
- [5] Gourev V N, Yordanov V G and Mishonov T M 2013 Measurement of the speed of light with an analytic scale *2nd Bulgarian National Congress on Physical Sciences (Sofia, 25–29 September)* (in Bulgarian)
- [6] Brezice G 2014 Determination of ε_0 as a maturity exam for gymnasium (high school) in Brezice Slovenia http://www2.arnes.si/~bivsic/fizika/vaje/laboratorijske_vaje_matura.pdf, Laboratorijske vaje za maturo, gimnazija.brezice@guest.arnes.si (in Slovenian)
- [7] Poston T 1973 Do-it-yourself catastrophe machine *Manifold* **14** 40–51
- [8] Yordanov V G, Gourev V N, Manolev S G, Varonov A M and Mishonov T M 2016 Measuring the speed of light with electric and magnetic pendulum arXiv:1605.00493 [physics.ed-ph]
- [9] Anonymous 2016 Private communication by an anonymous referee of the present work
- [10] Mishonov T M, Varonov A M, Maskimovski D D, Manolev S G, Gourev V N and Yordanov V G 2016 An undergraduate laboratory experiment on measuring the velocity of light with a catastrophic machine arXiv:1605.05218 [physics.ed-ph]
- [11] Landau L D and Lifshitz E M 1988 Gravitational collapse of a spherical body *The Classical Theory of Field (Course of Theoretical Physics vol 2)* 7th edn (Moscow: Nauka) section 102, problem 1, figures 21, 22
 Landau L D and Lifshitz E M 1988 Mendelev periodic system of elements *Quantum Mechanics —Non-Relativistic Theory (Course of Theoretical Physics vol 3)* 4th edn (Moscow: Nauka) section 73, there is a catastrophic fold for the integral from effective potential energy, equation (73.2)
 Landau L D and Lifshitz E M 1988 *Statistical Physics, Part 1 (Course of Theoretical Physics vol 5)* 5th edn (Moscow: Nauka) section 143 (Jump of heat capacity), figure 62, equation (143.5), section 144 (External field in influence on a phase transition), equation (144.4), figure 64
 Landau L D and Lifshitz E M 1988 *Fluid Mechanics (Course of Theoretical Physics vol 6)* 3rd edn (Moscow: Nauka) section 115 (Stationary simple waves), equation (115.9), section 119 (Solutions of Euler-Tricomi equation near non-singular points of the sound surfaces), equation (119.14)
 Landau L D and Lifshitz E M 1988 *Electrodynamics of Continuous Media (Course of Theoretical Physics vol 8)* 3rd edn (Moscow: Nauka) section 3 (Methods for solutions of electrostatic problems), problem 11 (Kirchhoff formula), section 5 (Forces acting on a conductor), section 30 (Magnetic field of a stationary currents), problem 2
 Landau L D and Lifshitz E M 1988 Ginzburg–Landau equations *Statistical Physics, Part 2 (Course of Theoretical Physics vol 9)* (Moscow: Nauka) section 45, equation (45.10)
 Landau L D and Lifshitz E M 1988 *Physical Kinetics (Course of Theoretical Physics vol 10)* (Moscow: Nauka) section 100 (Kinetics of type one phase transitions. Stadium of a coalescence), equation (100.9), section 101 (Relaxation of the order parameter near to the point of type two phase transition), equation (101.8–11)
 There are translations in many languages and many editions: Bulgarian, German, English, French, Japanese, Spanish..., but the cited numbers of sections, equations, figures and problems are translation invariant
- [12] Poston T and Stewart I N 1978 *Catastrophe Theory and its Applications* (London: Pitman) figures 2.8, 2.13, 2.14, 4.6, 5.4, 5.5, 5.6, 5.8, 5.9, 5.10, 5.11, 5.12, 5.15, 7.1, 7.5, 7.6, 7.7, 7.14, 8.8, 8.13, 9.2, 13.7, 13.41, 14.1, 14.2, 14.3, 14.4, 14.6, 14.10, 15.2, 15.4, 16.19, 16.20, 17.1, 17.6, 17.12, 17.13, 17.14, 17.15, 17.17, equations (2.7), (5.2), (5.4), (5.8), ch 6, section 2, ch 8, section 13, ch 9, section 3, (9.1), ch 14, section 1, section 2, section 7, section 8
- [13] Thom R 1972 *Stabilité Structurelle et Morphogénèse* (New York: Benjamin)
- [14] Zeeman C E 1972 A catastrophe machine *Towards a Theoretical Biology* 4 ed C H Waddington (Edinburgh: Edinburgh University Press) pp 276–82

- [15] Filippov B P 2007 *Eruptive Processes in the Sun* (Moscow: Fizmatlit) ch 4, figure 4.19 (in Russian)
- [16] Zeeman C E 1972 Differential equations for the heartbeat and nerve impulse *Towards a Theoretical Biology 4* ed C H Waddington (Edinburgh: Edinburgh University Press) pp 8–67
- [17] Arrowsmith D K and Place C M 1982 *Ordinary Differential Equations, A Qualitative Approach with Applications* (London: Chapman and Hall)
Arrowsmith D K and Place C M 1986 *Ordinary Differential Equations, A Qualitative Approach with Applications* (Mir: Moscow) (Russian translation)
- [18] Patashinski A Z and Pokrovsky V L 1979 Preface *Fluctuation Theory of Phase Transitions* (New York: Pergamon)
- [19] Damyanov D S, Pavlova I N, Ilieva S I, Gourev V N, Yordanov V G and Mishonov T M 2015 Planck's constant measurement by Landauer quantization for student laboratories *Eur. J. Phys.* **36** 055047
- [20] Frenet F 1847 Sur les courbes à double courbure *Thèse* Faculté des Sciences de Toulouse
Frenet F 1852 *J. Math.* **17** 437–47
- [21] Serret J A 1851 Sur quelques formules relatives à la théorie des courbes à double courbure *J. Math.* **16** 193–207